

# Land-Focused Changes in the Updated GEOS FP System (Version 5.25)

Randal D. Koster, Rolf H. Reichle, Sarith P. P. Mahanama, Justin Perket, Qing Liu, and Gary Partyka

## **SUMMARY**

Many of the changes imposed in the January 2020 upgrade from Version 5.22 to 5.25 of the Goddard Earth Observing System (GEOS) Forward Processing (FP) analysis system were designed to increase the realism of simulated land variables. The changes, which consist of both land model parameter updates and improvements to the physical treatments employed for various land processes, have generally positive or neutral impacts on the character of the FP product, as documented here.

## **BACKGROUND**

The land surface is a key component of a coupled Earth system model. Deficiencies in its representation can reduce the accuracy of other components of the system; accordingly, land model improvements should lead to improvements in the system as a whole. Known deficiencies in the GEOS land modeling system were previously corrected in the Soil Moisture Active Passive (SMAP) Level-4 production system hosted at GMAO (Reichle et al., 2017a, 2019). Almost all of these corrections, including improvements to prescribed parameter values and parameterizations, are now incorporated into the GEOS FP system, Version 5.25. This Research Brief documents the land-focused changes and their impact on the upgraded system.

## 1. Nature of Imposed Changes

The land model component of the GEOS FP system is the Catchment land surface model, or LSM (Koster et al., 2000; Ducharne et al., 2000). The Catchment LSM is a soil-vegetation-atmosphere transfer model that solves, at every time step, the surface energy and water balances within a number of surface reservoirs and accordingly provides the atmosphere with fluxes of latent and sensible heat appropriate for current weather conditions. As part of the recent GEOS FP upgrade from Version 5.22 to 5.25, a substantial number of modifications were imposed to the Catchment LSM's implementation in the system. These modifications fall into two broad categories: (a) changes to prescribed land model parameters and (b) changes to the land model parameterizations.

### a. Changes in prescribed land model parameters.

Many of the values used for land model parameters in the pre-upgrade FP system were out of date, sometimes being based on data collected and processed decades earlier. (See Reichle et al. [2017b] for a broader description of the pre-upgrade version of the land model.) The land model parameter values used now in Version 5.25 reflect more recent, higher resolution data collected with more advanced sensors. The new datasets, described in more detail by Mahanama et al. (2015), include:

(i) *Topography and Watersheds*. The basic land surface element utilized by the Catchment LSM is the hydrological catchment, an irregularly shaped area determined through the analysis of a digital elevation map (DEM). The pre-upgrade version of the FP system utilized catchments determined with a global, 1-km DEM (HYDRO1K; GTOPO30 1996). In Version 5.25 of the FP system, the catchments are derived (Verdin, 2013) from a much higher resolution (30 m) DEM produced by the Shuttle Radar Topography Mission (Slater et al., 2006). The higher resolution DEM data also provide improved catchment-specific spatial distributions of the compound topographic index, information that underlies the calculation of numerous critical model parameters (Ducharne et al., 2000).

(ii) *Soil Data*. Soil texture data in the pre-upgrade FP system were extracted from Reynolds et al. (2000). Version 5.25 utilizes the recent dataset from De Lannoy et al. (2014), which separates soil textures, accounting for relative carbon content, across the globe into 253 distinct types on a 1-km grid. Soil hydraulic properties, such as hydraulic conductivity, are in turn derived from these soil textures using pedotransfer functions rather than from simple look-up tables (as used in the pre-upgrade FP system).

(iii) *Leaf Area Index (LAI)*. LAI helps determine canopy conductance, and thereby evapotranspiration, in the Catchment LSM. In the pre-upgrade version of FP, LAI was assigned using AVHRR data (Dirmeyer and Oki, 2002). In Version 5.25, the prescribed seasonally varying LAI fields are obtained from a merging of MODIS (MODIS, 2008) and Geoland2 (Baret et al., 2012, Camacho et al., 2013) datasets. This combination takes advantage of the different strengths of these two more recent sources (Mahanama et al., 2015).

(iv) *Landcover*. The distribution of vegetation types in Version 5.25 of FP is based on the GlobCover v2.3 dataset (GLOBCOVER, 2011), a substantially newer and higher resolution dataset than that used in the pre-upgrade version (GLCC v2.0, 2000). While the distributions in the GlobCover v2.3 dataset are mapped, as before, into 6 basic types for use with the Catchment LSM, the areal coverages of these 6 types are considered more accurate in the upgraded system. One important facet of these new distributions is the associated land mask. For example, Figure 1 shows, for both the old and the new landcover descriptions, the prescribed distinction between land and water within a section of eastern Africa. The extensive water areas prescribed in the old system within the red rectangle are absent in the new system. Comparison with the satellite imagery indicates that the newer representation is indeed more accurate; the extraneous water bodies indicated by GLCC v2.0, if they ever do exist, are at best transient.

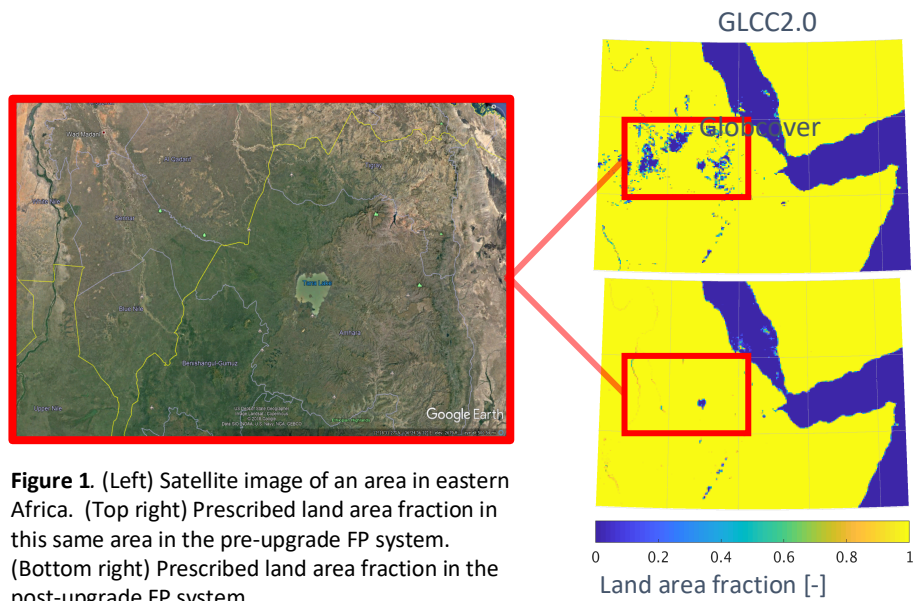


**Figure 1.** (Left) Satellite image of an area in eastern Africa. (Top right) Prescribed land area fraction in this same area in the pre-upgrade FP system. (Bottom right) Prescribed land area fraction in the post-upgrade FP system.

**b. Changes in model physics**

The FP upgrade includes a number of changes in the physical treatments of land surface processes. These changes were motivated by known issues with the earlier treatments; again, many of the strategies for improvement came about during the development of the SMAP Level 4 product (e.g., Reichle et al., 2019).

(i) *Snow Cover Fraction.* In the pre-upgrade system, snow cover fraction would increase linearly with snow water equivalent (SWE) until the SWE reached 26 kg/m<sup>2</sup> of water equivalent; thereafter, the Catchment land element was assumed to be fully snow-covered (though vegetation would still be allowed to “stick out” of the snow to affect the albedo). In the new system, the linear increase is faster, and the land element is assumed to be fully snow-covered when the SWE reaches half the earlier amount, 13 kg/m<sup>2</sup> of water equivalent. This has the effect of increasing snow cover in low snow conditions and is more consistent with MODIS observations of snow cover fraction (Toure et al., 2018).

(ii) *Heat Capacity of the Surface Soil Layer.* One undesirable feature of the pre-upgrade FP system is the potential for numerical instability in the surface energy budget calculations, an instability that can lead to unrealistic temperature oscillations from time step to time step. To address this problem, the new system features a surface soil layer with a larger heat capacity – whereas the pre-upgrade system used a soil heat capacity of 70,000 J kg<sup>-1</sup> K<sup>-1</sup> in tropical forests and 200 J kg<sup>-1</sup> K<sup>-1</sup> elsewhere, FP Version 5.25 uses a soil layer heat capacity of 70,000 J kg<sup>-1</sup> K<sup>-1</sup> everywhere. Numerous tests with the coupled GEOS land-atmosphere system confirmed that this increase considerably reduces the occurrence of unrealistic high frequency temperature oscillations.

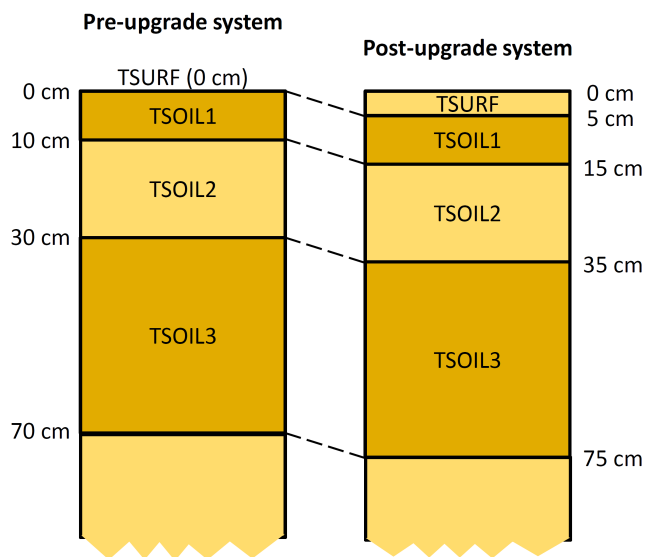


**Figure 2.** Effective change in the thickness and depths of the soil layers connected to the FP system’s land temperature variables. (Depths shown are approximate.)

In a sense, increasing the surface layer's heat capacity is equivalent to increasing the thickness of this layer, as illustrated in Figure 2. This change has implications for the interpretation of all FP soil temperature products – in areas outside of tropical forests, the depth at which each soil temperature value can be said to apply has been shifted downward by roughly 5 cm.

(iii) *Parameterization of Recharge into the Surface Soil Layer.* Koster et al. (2018) describe an analysis in which SMAP data are used to calibrate the parameterization of surface moisture recharge in the Catchment LSM. This analysis approach, with calibration against scattered in situ soil moisture measurements, led to a modification in the Catchment LSM's recharge formulation that was incorporated into the SMAP Level 4 production system and is now a part of FP Version 5.25. In essence, through this change, upward flow into the surface soil layer is more restricted, leading to a generally drier soil surface, which is generally more consistent with independent in situ soil moisture measurements (Reichle et al., 2019).

(iv) *Surface Roughness.* The aforementioned changes in the vegetation landcover maps and LAI distributions already have a first order impact on the aerodynamic surface roughness values used in the upgraded FP system. In addition to these changes, FP Version 5.25 includes a higher minimum surface roughness (which particularly affects turbulent fluxes in deserts) and applies estimates of stem area index along with leaf area index in the roughness calculation.

## **2. Impact of Changes on Simulated Land Variables**

The character of the land surface fields generated by the GEOS FP system has changed with the upgrade, sometimes in significant ways. In general, changes in the simulated fields are either improved relative to observations or are essentially neutral, with improvements in some locations balanced by degradations in others.

In the following, the performance of the upgraded land model is investigated using two different test simulations. The first experiment is a 1-year (~2018) 3D-Var analysis using an intermediate version of the GEOS AGCM (atmospheric general circulation model) at ½-degree resolution coupled to the updated land model. The results from this experiment are compared to those from an equivalent analysis using the same atmospheric system

and the previous version of the Catchment LSM. The second experiment is the FP “parallel” (FPP) operational run for October 2019 through January 2020 using the full hybrid, 4D-EnVar analysis with the updated AGCM at 1/8-degree resolution; here, results are compared to the full pre-upgrade FP system. The first comparison isolates improvements directly attributable to the updated Catchment LSM; the second comparison captures the additive effects of both atmospheric and land improvements.

The changes in the upward recharge parameterization and the soil properties result in generally drier – and improved – surface soil moisture conditions (De Lannoy et al., 2014, Reichle et al., 2019). Figure 3 shows some results from the first experiment described above: the root-mean-square error (RMSE) between the surface moisture generated in the analysis system (both before and after the land model upgrade) and the Level 2 retrievals provided by the SMAP mission (computed across the globe where SMAP Level 2 soil moisture data are available). The RMSE in the new system is reduced by a significant fraction – small degradations in the Sahel are more than counterbalanced by improved soil moisture simulation in the western US, eastern Asia, eastern and southern Africa, and most of South America (not shown).

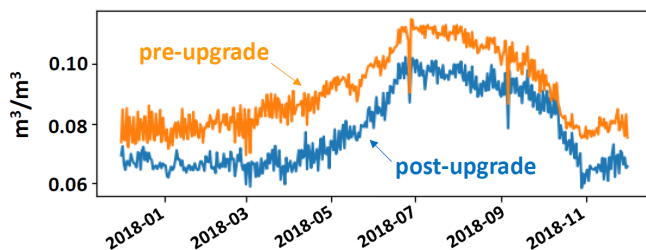


**Figure 3.** RMSE, vs. SMAP Level 2 observations, of surface soil moisture data generated by experimental versions of the pre-upgrade (orange) and post-upgrade (blue) FP system.

The first experiment also produced the closeness plot for runoff ratio (the fraction of incident precipitation water that runs off the surface rather than infiltrates and later evaporates) shown in Figure 4. The closeness plot shows improvements across the continental US. Here the observations are naturalized stream gauge measurements, as described in Mahanama et al. (2012). Runoff ratios produced with the updated land model are still lower than observations-based estimates, but the imposed changes, particularly in the parameterization of surface recharge, do increase the ratios, moving them in the right direction.

The second experiment described above provided the data used to evaluate the impacts of the FP upgrades on 2-m air temperature (T2M). The differences plotted are thus not solely a result of the imposed land surface changes; to some extent, they also reflect changes in modeled rainfall and radiation. With this in mind, consider Figure 5 (left), which shows the average difference in T2M between the two systems for the period October 2019 - January 2020, when the full pre-upgrade and post-upgrade FP systems ran in parallel. Tropical temperatures are reduced in Version 5.25, by multiple degrees in some places. Some higher latitude areas, including the Arctic, northeast Canada, and northeast Eurasia, also show T2M reductions in Version 5.25; however, by and large, subtropical and midlatitude temperatures have increased. A closeness plot is provided in the right panel of Figure 5, with ECMWF (European Centre for Medium-range Weather Forecasts) T2M used for comparison. The closeness plot shows a mixture of improvements and degradations (relative to ECMWF) with the new system. On balance, according to this metric, the impacts of the system upgrades on T2M are neutral.

Runoff Ratio: Abs(Post-upgrade Error) minus Abs(Pre-upgrade Error)

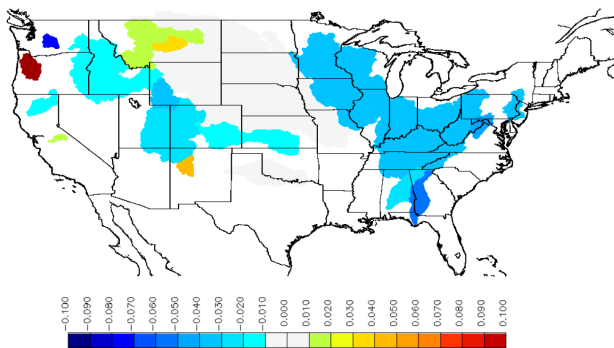


**Figure 4.** Closeness plot comparing the (absolute) error in runoff ratio for 2018 between experimental versions of the pre-upgrade and post-upgrade systems. Truth here was obtained from long-term (multi-decadal) climatologies of rainfall and streamflow in the basins examined, each derived from in situ measurements. Blue colors indicate that the new system performs better.

The second experiment described above provided the data used to evaluate the impacts of the FP upgrades on 2-m air temperature (T2M). The differences plotted are thus not solely a result of the imposed land surface changes; to some extent, they also reflect changes in modeled rainfall and radiation. With this in mind, consider Figure 5, which shows the average difference in T2M between the two systems for the period October 2019 - January 2020, when the full pre-upgrade and post-upgrade FP systems ran in parallel. Tropical temperatures are reduced in Version 5.25, by multiple degrees in some places. Some higher latitude areas, including the Arctic, northeast Canada, and northeast

Eurasia, also show T2M reductions in Version 5.25; however, by and large, subtropical and midlatitude temperatures have increased. A closeness plot is provided in the right panel of Figure 5, with ECMWF (European Centre for Medium-range Weather Forecasts) T2M used for comparison. The closeness plot shows a mixture of improvements and degradations (relative to ECMWF) with the new system. On balance, according to this metric, the impacts of the system upgrades on T2M are neutral.

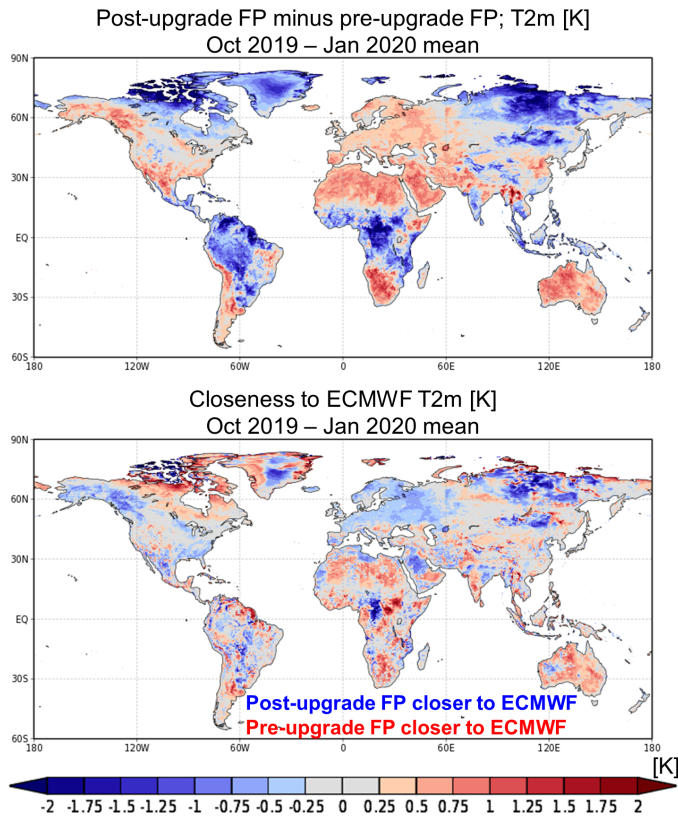


**Figure 5.** a) Differences (post-upgrade minus pre-upgrade) in simulated 2-meter air temperature averaged over October through January. b) Closeness plot indicating the degree to which the newer system improves over the older one, under the assumption that ECMWF fields represent truth. Blue colors indicate that the newer system performs better.

### 3. Discussion

The land-focused changes incorporated into the recently upgraded GEOS FP system (Version 5.25) have several advantages. First, they allow the FP system to make use of more recent, more highly resolved, and generally more accurate land surface parameter fields, many of which were derived from NASA remote-sensing missions. Second, they correct some known deficiencies in the land modeling system, such as oscillations in soil surface temperature stemming from numerical instabilities. Third, they synchronize the



GEOS FP system and the SMAP Level 4 production system; with the two systems now using similar versions of the land model, GMAO expenditures in land model maintenance are reduced. Finally, and perhaps most importantly, the imposed changes lead to improvements in some model fields (e.g., soil moisture, surface runoff) while producing essentially neutral changes in others (e.g., near-surface air temperature). The improvements that do exist are expected to increase overall GEOS FP performance.

Land model development, of course, continues in the GMAO, with parameterizations being developed and evaluated for (among other things) interannually varying vegetation properties, peatland hydrology, and permafrost dynamics. The natural expectation is that these developments too will eventually find their way into a future GEOS FP system.

## References

Baret, F., M. Weiss, R. Lacaze, F. Camacho, H. Makhmara, P. Pacholczyk and B. Smets, 2012: GEOV1: LAI, FAPAR Essential Climate Variables and FCOVER global time series capitalizing over existing products, Part 1, Principles of development and production. *Remote Sens. Environ.*, **137**, 299-309, doi:10.1016/j.rse.2012.12.027

Camacho, F., J. Cernicharo, R. Lacaze F. Baret, M. Weiss, 2013: GEOV1: LAI, FAPAR Essential Climate Variables and FCover global time series capitalizing over existing products, Part 2, Validation and inter-comparison with reference products. *Remote Sens. Environ.*, **137**, 310–329, doi:10.1016/j.rse.2013.02.030

De Lannoy, G. J. M., R. D. Koster, R. H. Reichle, S. P. Mahanama, and Q. Liu, 2014: An updated treatment of soil texture and associated hydraulic properties in a global land modeling system. *J. Adv. Model. Earth Syst.*, **06**, doi:10.1002/2014MS000330

Dirmeyer, P. and T. Oki, 2002: The Second Global Soil Wetness project (GSWP-2) Science 2 and Implementation Plan. IGPO Publication Series No. 37, 64p.

Ducharne, A., R. D. Koster, M. J. Suarez, M. Stieglitz, and P. Kumar, 2000: A catchment-based approach to modeling land surface processes in a general circulation model, 2, Parameter estimation and model demonstration. *J. Geophys. Res.*, **105**, 24823-24838.

GLCC v2, 2000: Global Land Cover Characteristics Data Base Version 2.0 (Available at [ftp://edcftp.cr.usgs.gov/data/glcc/globdoc2\\_0.html](ftp://edcftp.cr.usgs.gov/data/glcc/globdoc2_0.html))

GLOBCOVER, 2011: GLOBCOVER 2009, Products Description and Validation Report. ESA Technical Note. (Available [http://due.esrin.esa.int/files/GLOBCOVER2009\\_Validation\\_Report\\_2.2.pdf](http://due.esrin.esa.int/files/GLOBCOVER2009_Validation_Report_2.2.pdf).)

GTOPO30, 1996: GTOPO30 - Global Topographic Data. U.S. Geological Survey, EROS Data Center Distributed Active Archive Center (EDC DAAC), Available at <https://lta.cr.usgs.gov/GTOPO30>, USA.

Koster, R. D., M. J. Suarez, A. Ducharne, M. Stieglitz, and P. Kumar, 2000: A catchment-based approach to modeling land surface processes in a general circulation model, 1, Model structure. *J. Geophys. Res.*, **105**, 24809-24822.

Koster, R. D., Q. Liu, S. P. Mahanama, and R. H. Reichle, 2018: Improved hydrological simulation using SMAP data, Relative impacts of model calibration and data assimilation. *J. Hydromet.*, **19**, 727-741, doi: 10.1175/JHM-D-17-0228.1.

Mahanama, S., B. Livneh, R. Koster, D. Lettenmaier, and R. Reichle, 2012: Soil moisture, snow, and seasonal streamflow forecasts in the United States. *J. Hydromet.*, **13**, 189-203, doi: 10.1175/JHM-D-11-046.1.

Mahanama, S. P., R. D. Koster, G. K. Walker, L. L. Takacs, R. H. Reichle, G. De Lannoy, Q. Liu, B. Zhao, and M. J. Suarez, 2015: Land boundary conditions for the Goddard Earth Observing System Model Version 5 (GEOS-5) climate modeling system—Recent updates and data file descriptions. NASA/TM–2015-104606, Vol. 39, 55 pp. Document (4608 kB).

MODIS, 2008: MOD15A2 v005. NASA EOSDIS Land Processes DAAC, USGS Earth Resources Observation and Science (EROS) Center, Sioux Falls, South Dakota (<https://lpdaac.usgs.gov>); data accessible at <http://e4ftl01.cr.usgs.gov/MOLT/MOD15A2.005/>.

Reichle, R. H., and Coauthors, 2017a: Assessment of the SMAP Level-4 Surface and Root-Zone Soil Moisture Product Using In Situ Measurements. *J. Hydromet.*, **18**, 2621-2645, doi:10.1175/JHM-D-17-0063.1.

Reichle, R. H., C. S. Draper, Q. Liu, M. Girotto, S. P. P. Mahanama, R. D. Koster, and G. J. M. De Lannoy, 2017b: Assessment of MERRA-2 land surface hydrology estimates, *J. Climate*, **30**, 2937-2960, doi:10.1175/JCLI-D-16-0720.1.

Reichle, R. H., and Co-authors, 2019: Version 4 of the SMAP Level-4 Soil Moisture Algorithm and Data Product. *J. Adv. Model Earth Syst.*, **11**, 3106-3130, doi:10.1029/2019MS001729.

Reynolds, C. A., T. J. Jackson, and W. J. Rawls, 2000: Estimating soil water-holding capacities by linking the Food and Agriculture Organization Soil map of the world with global pedon databases and continuous pedotransfer functions. *Water Resour. Res.*, **36**(12), 3653-3662, doi:10.1029/2000WR900130.

Slater, J. A., G. Garvey, C. Johnston, J. Haase, B. Heady, G. Kroenung, and J. Little, 2006: The SRTM data "finishing" process and products. *Photogramm. Eng. Remote Sens.*, **72**, 237-247, doi:10.14358/pers.72.3.237.

Toure, A. M., R. H. Reichle, B. A. Forman, A. Getirana, and G. J. M. De Lannoy, 2018: Assimilation of MODIS Snow Cover Fraction Observations into the NASA Catchment Land Surface Model. *Remote Sens.*, **10**, 316, doi:10.3390/rs10020316.

Verdin, K., 2013: Final Report: High Resolution Topographic Analysis for GMAO's Catchment LSM, pp21. Available at Global Modeling and Assimilation Office, Code 610.1, NASA/Goddard Space Flight Center, Greenbelt, MD 201771.